

Chemistry Using Coulomb Crystals

Brianna R. Heazlewood[†] and Heather J. Lewandowski^{*,‡,§}

[†]Department of Physics, University of Liverpool, Liverpool L69 7ZE, United Kingdom

[‡]Department of Physics, University of Colorado, Boulder, Colorado 80309, United States

[§]JILA, National Institute of Standards and Technology and University of Colorado, Boulder, Colorado 80309, United States

*Email: lewandoh@colorado.edu.

Laser cooling of atomic ions has long been used as a tool in physics to explore quantum entanglement for applications in quantum computing and information. More recently, laser-cooled atomic ions have been used as a platform for studying cold chemistry. Here, we describe an experimental system called a “Coulomb crystal,” where laser-cooled ions are confined in traps at sufficiently low translational energies that they form an ordered structure. We then present a range of experiments undertaken using this platform, from studies of reactions with an atomic species to reaction systems of increased complexity, involving molecular ions and neutral molecules. We also describe a few spectroscopic studies enabled by Coulomb crystals before discussing some possible future directions of the field. This is not meant to be a comprehensive review of the entire field, but rather a sampling of the types of experiments that can be performed and the knowledge gained from these studies.

Introduction

Laser cooling of atomic ions has long been used as a tool in physics to explore quantum entanglement for applications in quantum computing and information (1). More recently, laser-cooled atomic ions have been used as a platform for studying cold chemistry (2–12). Here, we describe an experimental system called a “Coulomb crystal,” where laser-cooled ions are confined in traps at sufficiently low translational energies that they form an ordered structure. We then present a range of experiments undertaken using this platform, from studies of reactions with an atomic species to reaction systems of increased complexity, involving molecular ions and neutral molecules. We also describe a few spectroscopic studies enabled by Coulomb crystals before discussing some possible future directions of the field. This is not meant to be a comprehensive review of the entire field, but rather a sampling of the types of experiments that can be performed and the knowledge gained from these studies.

There are a number of advantages associated with using Coulomb crystals for chemical reaction studies. First and foremost, Coulomb crystals enable ionic species to be cooled to translational temperatures of ~ 10 mK to 10 K (as detailed in the following sections), creating a dense and localised target of trapped reactants. Such environments allow laboratory-based reaction studies to be carried out in conditions comparable to those found in remote regions such as the interstellar medium (ISM). The high degree of control that can be exerted over the trapped reactants, and the range of complementary detection methods available, are also beneficial for the study of fundamental chemical reactivity. The ultra-high vacuum conditions and long trapping times (up to hours) make it possible to study slow or infrequent processes with high sensitivity. Finally, in many cases, the ionic products of ion-neutral reactions studied in Coulomb crystals can be confined and accumulated in the trap—allowing product formation to be directly monitored.

Coulomb Crystals

A Coulomb crystal is an ensemble of cold, tightly-confined ions. Upon laser cooling, trapped and translationally cold ions can adopt an ordered lattice-like (or “crystalline”) structure. Linear Paul ion traps are commonly used to confine the ions, although other trap designs (such as Penning traps) can also be employed (5). A Coulomb crystal is formed when sufficient kinetic energy has been removed from the trapped ions, such that the potential energy of the ions far exceeds their kinetic energy: $E_{pot}/E_{kin} \gtrsim 160$ (13, 14). The combination of confining forces imposed by the trapping fields and repulsive Coulombic forces between neighbouring ions gives rise to a periodic arrangement of ions. Neighbouring ions are typically separated by 10–20 μm , with a density on the order of 10^8 ions cm^{-3} (4, 6, 10). Coulomb crystals can adopt a number of different shapes—from one-dimensional strings to three-dimensional spheroidal or spherical structures—depending on the number of trapped ions and the trapping potential. Most of the studies discussed in this chapter involve spheroidal crystals, containing between a few hundred and a few thousand ions.

Laser-cooling schemes have been implemented for the alkaline earth metal cations (Be^+ , Mg^+ , Ca^+ , Sr^+ , Ba^+ , Ra^+) and species such as Yb^+ , providing a highly efficient means of removing kinetic energy from these trapped ions (15–17). A frequently adopted laser-cooling scheme for Ca^+ ions requires only two diode lasers: one to excite the $4s\ ^2S_{1/2} \rightarrow 4p\ ^2P_{1/2}$ transition and the other to pump population out of the metastable $3d\ ^2D_{3/2}$ state, returning it to the main cooling cycle. However, there are experimental challenges that make laser cooling impractical for the vast majority of ionic species beyond the ones mentioned above. This is particularly true for molecular ions, where the complex energy level structure (arising from the additional vibrational and rotational states) requires multiple lasers to address population lost to states outside the main cooling cycle. Ionic species that are not amenable to laser cooling can instead be “sympathetically cooled” into a Coulomb crystal, where the cooling impacts only the translational motion of the co-trapped ions. Sympathetic cooling occurs when co-trapped ions undergo elastic collisions with laser-cooled ions, and is most efficient when the collision partners have similar mass-to-charge ratios. It is therefore important to consider the properties of the target ionic species when selecting an appropriate laser-cooled species. For example, Be^+ ions are an obvious choice when one wishes to co-trap ions with low mass-to-charge ratios. For studies involving heavier ions, laser-cooled Ba^+ ions are often required. As will be seen in the subsequent sections of this chapter, a diverse range of ionic species have now been incorporated into multi-component Coulomb crystals.

In addition to removing kinetic energy from the trapped ions, the laser-cooling cycle also makes it possible for ion lattice positions to be directly observed. The fluorescence emitted by laser-cooled ions as they return to the ground electronic state can be imaged with a microscope objective and recorded with a camera, facilitating direct observation of the average locations of laser-cooled ions within the crystal. It should be noted that individual ions are (typically) not directly observed, as the ions within the crystal are constantly exchanging positions. Rather, it is the lattice positions of the trapped ions—their average locations within the crystal framework—that is captured. Experimental images of the central slice of a spheroid-shaped Coulomb crystal are shown in Figure 1. While it is not possible to directly observe any sympathetically-cooled ions in the crystal (as these species do not fluoresce), their presence can be indirectly established from the positions of laser-cooled ions. As the confining forces experienced by trapped ions depend on their mass-to-charge ratios, different ionic species will localise in different regions of the trap in multi-component crystals. In this way, species with lower mass-to-charge ratios will localise along the central axis of the trap (giving rise to a dark core, when these species are sympathetically cooled). Figure 1 shows the changes in the fluorescing Ca^+ framework when different numbers of Xe^+ and ammonia ions are present in the crystal (18).

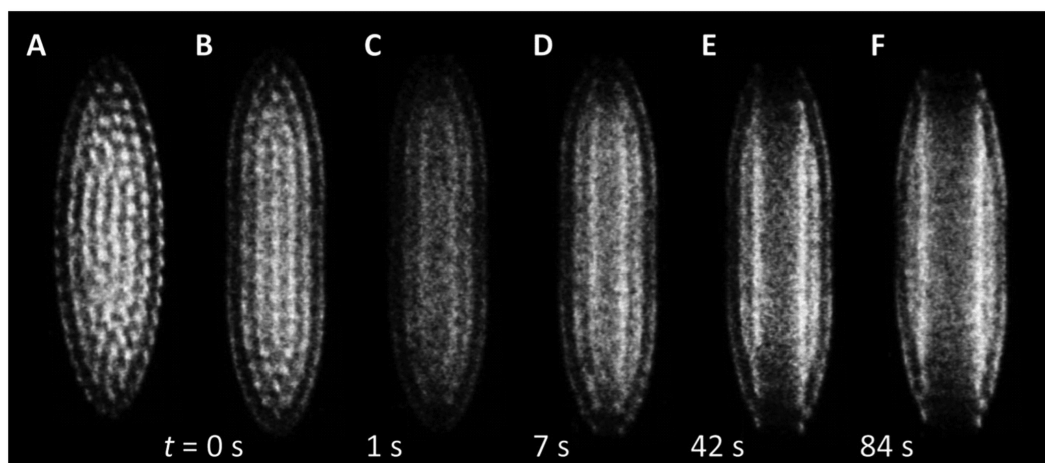


Figure 1. Experimental images of the central slice of a three-dimensional Coulomb crystal. (A) Shows a Coulomb crystal containing only laser-cooled Ca^+ ions. In image (B), sympathetically-cooled Xe^+ ions have been incorporated into the crystal. While the Xe^+ ions cannot be directly imaged (they are not laser cooled, and so do not fluoresce), their presence can be seen in the characteristic flattening of the lattice positions of the Ca^+ ions in the crystal. Images (C) to (F) show the progress of a charge transfer reaction between Xe^+ ions and neutral ammonia molecules, with the formation of ammonia ions able to be observed through the growth of a dark core in the centre of the crystal. Reproduced with permission from reference (18).

Copyright 2015 American Chemical Society.

Reaction Studies

Lasers play a number of important roles in the study of reactions using Coulomb crystals. In particular, lasers can be used to form ionic reactants, laser-cool trapped ions, state-select reactants, initiate reactions, and probe ionic reaction products. The first reaction involving Coulomb-crystallized ions was reported in 2000, involving an atomic ion and diatomic neutral molecule: $\text{Mg}^+ + \text{H}_2 \rightarrow \text{MgH}^+ + \text{H}$ (19). In the decades since this first study, advances in detection methods have seen reactions of increasing complexity examined within Coulomb crystals. Reaction systems

featuring polyatomic reactants and multiple competing product channels have been successfully studied, enabling reaction rate coefficients and branching ratios to be established, as well as elucidating reaction mechanisms. In this section, the ways in which lasers facilitate the study of reactions in Coulomb crystals will be presented, alongside a discussion of the chemistry that has been uncovered.

Processes Involving an Atomic Reactant

Reactions of Laser-Cooled Ions

The earliest reaction studies in Coulomb crystals focused on processes involving laser-cooled ions: systems where (predominantly) Be^+ , Mg^+ , Ca^+ or Ba^+ ions were the ionic reactants. There are several reasons why understanding the reactions of laser-cooled ions are of interest. In some cases—especially for reactions involving Be^+ and small molecules such as H_2 —the reactions are directly relevant to the chemistry occurring in the ISM (20). In other cases—for example, in the reaction of Ca^+ with CH_3F —experimental measurements enabled theories of reactivity to be challenged and the importance of certain features of the underlying potential energy surfaces (PESs) to be established (21). In all cases, quantifying the reactivity of laser-cooled ions with any neutral reactant of interest is an important first step before the reactions of other co-trapped ionic species can be considered. This is because the presence of laser-cooled ions is a prerequisite for forming Coulomb crystals; it's important to know how quickly the laser-cooled ions might react with neutral molecules of interest, as these reactions must be accounted for in any subsequent analysis involving co-trapped ionic reactants. (For example, H_2O reacts readily with Be^+ (22) but more slowly with Ca^+ . As such, examining the reactions of co-trapped ions with H_2O is more straightforward in Ca^+ Coulomb crystals than in Be^+ crystals.)

Examining the reactivity of laser-cooled ions may initially appear to be straightforward. In one sense, it is; no other ionic reactants need to be introduced, as the laser-cooled ions that make up the observable framework of the Coulomb crystal are also the ionic reactants. However, extracting properties such as state-specific rate coefficients from these studies is often far from simple. This is because of the multiple electronic states that are populated as part of the laser-cooling process. For example, the laser cooling scheme for Ca^+ ions introduced earlier in this chapter populates three electronic states: the ground ($^2\text{S}_{1/2}$) state and two excited ($^2\text{P}_{1/2}$ and $^2\text{D}_{3/2}$) states. In some reaction systems, the process of interest is only energetically accessible when ions are in the highest-energy state ($^2\text{P}_{1/2}$ for Ca^+ reacting with neutral NO) (23). There are, however, numerous examples of systems where more than one electronic state can give rise to reaction products; frequently, two or more excited states populated during the laser cooling cycle lead to exothermic reaction channels. To ascertain the contribution of each electronic state to the experimentally observed rate coefficient, it is necessary to vary the population in each of the reactive electronic states in a controlled manner—such as by adjusting the de-tuning of the cooling laser(s). The Optical Bloch Equations can then be employed to estimate the relative population of each electronic state (21, 24). By undertaking measurements at a range of different population distributions, reaction rate coefficients for each state can be determined.

Numerous reactions involving laser-cooled ions have been studied in Coulomb crystals. These include the reactions of Be^+ with H_2 , HD , D_2 and H_2O (20, 22); of Mg^+ with H_2 and D_2 (19); of

Ca⁺ with Li, K, Rb, H₂, NO, O₂, H₂O, HOD, N₂O, ND₃, CH₃F, CH₂F₂, CH₃Cl, CH₃CN and 3-aminophenol (21, 23–34); of Ba⁺ with O₂, Br₂, CO₂, N₂O, CH₃Cl, CH₃OH and SF₆ (35–38); of Yb⁺ with Li, Ca and Rb (38–40); and very recently, of Ra⁺ with CH₃OH (41). Many of these studies have been discussed in depth in earlier review articles, and so will not be covered in detail in this chapter (2–6, 10–12). It should be noted, however, that a number of these systems display interesting chemical reaction dynamics. The classical picture that one might conjure for a barrierless reaction pathway—where the colliding reactants simply roll down a potential energy hill to form products—frequently oversimplifies the chemistry. For example, the presence of features such as submerged barriers can give rise to experimental rate coefficients that are lower than predicted by capture theory calculations, even in “simple” reactions involving an atomic ion and a small molecular neutral reactant (21, 22).

Reactions of Co-trapped Atomic Ions

Moving beyond processes that involve laser-cooled ions, other ionic species can be sympathetically cooled into Coulomb crystals and their reactions studied. A number of charge transfer reactions have been examined with co-trapped, sympathetically cooled atomic ions. For example, the charge transfer reaction $\text{Mg}^{2+} + \text{O}_2 \rightarrow \text{Mg}^+ + \text{O}_2^+$ has been studied in a Mg⁺ Coulomb crystal. Both product ions have mass-to-charge ratios that enabled them to be confined by the trapping potential (and subsequently incorporated into the crystal). However, the exothermicity of the reaction (~2.8 eV) significantly exceeded the depth of the trap (~1.0 eV). Thus, the majority of product ions were imparted with > 1 eV of kinetic energy and therefore were able to escape from the trap volume (42). As few product ions were trapped, the reaction was studied by measuring the loss of reactant ions. The reaction between Ne⁺ ions and CH₃CN molecules has also been studied in a Ca⁺ Coulomb crystal by monitoring the loss of Ne⁺ reactant ions (43). While monitoring the consumption of the ionic reactant can provide important details about the overall reactivity of the system, reaction studies are even more powerful when combined with the knowledge of what products are formed.

For the charge-transfer reactions between rare-gas ions (Ar⁺, Kr⁺ and Xe⁺) and two isotopologues of ammonia (NH₃ and ND₃), all product ions were able to be confined by the trapping fields. This is because the reaction exothermicities of ≤ 5.6 eV were well within the trap depth of ≥ 6.3 eV for the ammonia product ions (44, 45). The charge-transfer reactions were studied using Ca⁺ Coulomb crystals, with neutral rare-gas atoms admitted to the reaction chamber and subsequently ionised using appropriate resonance-enhanced multiphoton ionisation (REMPI) schemes to generate the ionic reactants. The reaction progress was observed visually (by monitoring changes in the locations of fluorescing Ca⁺ ions in the crystal) and through time-of-flight mass spectrometry (ToF-MS) measurements, where both the reactant and product ions were detected.

When examining the experimental rate coefficients for the charge-transfer reactions of rare-gas ions with ammonia isotopologues, an unexpected inverse kinetic isotope effect (KIE) was observed: ND₃ was found to react faster than NH₃. Capture theory calculations could not account for the presence of inverse KIEs or the magnitude of the experimentally measured rate coefficients in any of the (Ar⁺, Kr⁺ or Xe⁺) charge-transfer systems investigated. Detailed theoretical work established that there were no energetically accessible crossing points between the product and reactant potential energy surfaces, indicating that charge transfer is not straightforward in these systems. It is proposed

that the efficiency of non-adiabatic coupling between the reactant and product surfaces, in addition to the properties of the reaction complex, play important roles in determining the likelihood of charge transfer occurring (45). While further work is required to confirm the validity of the proposed explanation, the experimental findings indicate that caution should be employed when using capture theories to estimate rate coefficients in the absence of any supporting experimental data. This is especially important in the context of astrochemical models, as many of the databases developed to describe the chemistry of the ISM are heavily dependent on capture-theory-based estimates of reactivity.

In another study examining processes relevant to astrochemistry, the reaction of C^+ ions with H_2O molecules was studied in Be^+ Coulomb crystals (46). The ionic species were formed by laser ablation of neutral Be and graphite, with the C^+ ions subsequently sympathetically cooled by the laser-cooled Be^+ ions. As the neutral reactants were buffer-gas cooled prior to being admitted to the ion trap chamber, the reaction was able to be studied under conditions comparable to those seen in cold interstellar clouds (~ 20 K). The $C^+ + H_2O$ reaction yields either HCO^+ or $HO C^+$ product ions (alongside an H atom), with these two product channels indistinguishable by mass spectrometry. The enhanced reactivity of $HO C^+$ ions was exploited, as only this isomer undergoes further reactions with N_2 to form $N_2^+ CO$ products. (Note that, to further separate the final product mass channels, $^{15}N_2$ was used in place of $^{14}N_2$.) Aided by this secondary reaction, the HCO^+ and $HO C^+$ product channels were able to be distinguished using ToF-MS detection methods, allowing the branching ratio of HCO^+ to $HO C^+$ formation to be ascertained (46).

Other Reactions Involving Atomic Species

Technical advancements have seen the combination of ion traps with traps for neutral species. In these “hybrid” trap set-ups there is spatial overlap between the two trapping volumes, enabling the species held within each trap to interact at very low collision energies. Collisions have been studied between a range of trapped ions (in Coulomb crystals confined within an ion trap) and ultracold atoms (in a magneto-optical trap, MOT). Many of these collisions—especially those occurring between atomic ions and atoms—involve elastic or inelastic scattering, where energy is transferred between the collision partners, but there is no change to the chemical identities of the species. As we are focusing on how lasers facilitate ion-neutral chemical reactions, non-reactive collisions fall outside the scope of this chapter. More details on inelastic scattering in hybrid traps can be found in a recent review paper (47).

Reactive collisions can also occur in hybrid traps, with some interesting chemical behaviour observed in the ion-atom reaction systems examined. While the collision energy is typically very low (from ~ 10 K down to a few mK), the neutral atomic reactant is frequently in an excited electronic state. As described above with laser-cooled ions within Coulomb crystals, the laser cooling of atoms confined in the MOT populates excited electronic states. As such, there can be a significant amount of internal energy in the colliding reactants—even though there is very little kinetic energy in the system. The synthesis of a hypermetallic alkaline earth oxide $BaOCa^+$ illustrates how, in some cases, it is necessary to consider additional excited states besides those directly involved in the laser cooling cycle (37). The formation of $BaOCa^+$ involved several steps. In the first instance, CH_3OH molecules were admitted to a reaction chamber containing a Ba^+ Coulomb crystal, resulting in the formation of sympathetically cooled $BaOCH_3^+$ ions (with other product ions resonantly excited and thereby

removed from the crystal). The trapped BaOCH_3^+ ions were then overlapped with ultracold Ca atoms confined in a MOT (or magnetic trap), with the formation of BaOCa^+ products confirmed by ToF-MS measurements (37). While the $\text{BaOCH}_3^+ + \text{Ca} (^1\text{S}_0) \rightarrow \text{BaOCa}^+ + \text{CH}_3$ reaction is exothermic, an intrinsic reaction coordinate calculation identified a significant reaction barrier (of approximately 10 kcal/mol) along the reaction pathway (see Figure 2). This implied that Ca reactants needed to be in an excited state for the reaction to proceed and yet, tuning the parameters of the MOT lasers, thereby modifying the relative populations of the various excited singlet states populated as part of the laser cooling cycle, did not change the overall reaction rate coefficient.

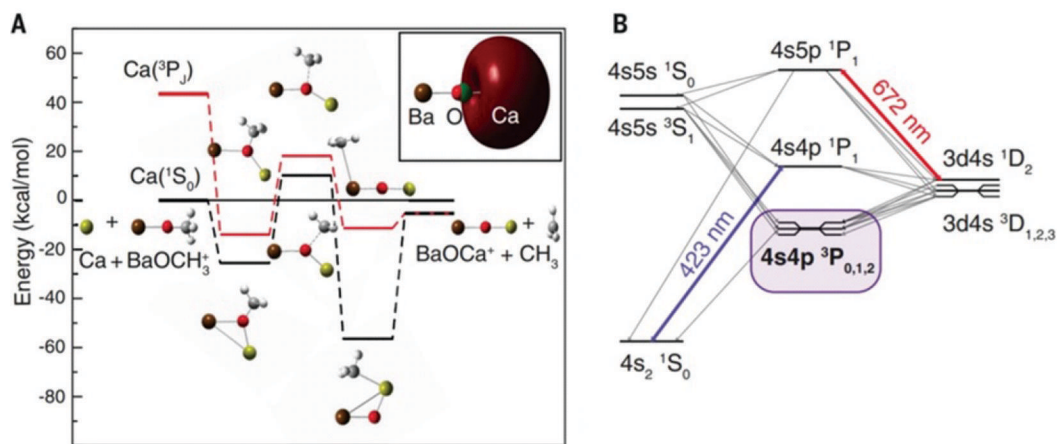


Figure 2. (A) The energies of stationary points along the reaction pathways involving $\text{Ca} (^1\text{S}_0)$ (in black) and $\text{Ca} (^3\text{P}_j)$ (in red) proceeding to BaOCa^+ products are indicated, calculated using the CCSD(T) method and a *cc-pV5Z* basis set. Note the presence of an energetic barrier to reaction in the $\text{Ca} (^1\text{S}_0)$ pathway. There is only a submerged barrier for reaction with $\text{Ca} (^3\text{P}_j)$. (B) Ca energy level diagram, with the states involved in the laser cooling scheme indicated. The reaction $\text{Ca} (^3\text{P}_j)$ states are indicated in bold text and highlighted. Reproduced with permission from reference (37). Copyright 2017 American Association for the Advancement of Science.

When exploring possible explanations for why the rate coefficient was unchanged when the populations of different excited states involved the laser cooling cycle were modified, the authors recalled some interesting findings from the 1990s. It was previously reported that spin-forbidden transitions from the excited singlet states of Ca (populated during the laser cooling process) could produce Ca atoms in the triplet (^3P) states (see Figure 2) (48). While metastable triplet Ca atoms are not confined by the MOT, their continuous production (albeit in small numbers) was sufficient for the reaction to proceed. Theory calculations confirmed that the $\text{BaOCH}_3^+ + \text{Ca} (^3\text{P}_j) \rightarrow \text{BaOCa}^+ + \text{CH}_3$ reaction is indeed energetically accessible, featuring only a submerged barrier. Reactions with Ca in the singlet excited states were proposed to feature energetic barriers (as seen with ground state Ca). Additional measurements involving triplet Ca atoms held in a magnetic trap confirmed the validity of the proposed mechanism, with the rate coefficient exhibiting a linear dependence on the number of $\text{Ca} (^3\text{P}_j)$ atoms in the trap as anticipated (37). The fact that this reaction was able to be detected—with the presence of very few reactant species in the trap volume—demonstrates the extreme sensitivity of the approach and the benefits of conducting experiments where product ions

can be trapped and the reaction process can be closely monitored. It also reinforces the importance of considering a range of possible excited-state pathways when examining the reactions of laser-cooled species.

Several other interesting reaction processes involving atomic species have been examined in hybrid traps. Low-energy reactive collisions have been studied between BaCl^+ ions and electronically excited Ca ($^1\text{P}_1$) atoms. Over the collision energy range 0.3–2 K, the reaction rate coefficient was found to decrease with decreasing temperature—in contrast to expectations from capture-theory calculations. The experimental observations were rationalised by consideration of a competing process: radiative decay of the Ca ($^1\text{P}_1$) reactants, producing (unreactive) ground state Ca atoms (49).

Finally, charge-transfer reactions $\text{Rb} + \text{O}_2^+$ and $\text{Rb} + \text{N}_2^+$ have also been studied in a hybrid trap set-up at low collision energies (50). With both ground state ($^2\text{S}_{1/2}$) and excited state ($^2\text{P}_{3/2}$) Rb atoms (populated by the MOT cooling lasers) able to react with the trapped molecular ions, nine energetically accessible product channels were identified in each system. The multiple close-lying product states arise because of the open shell nature of the reactants. Detailed theory work revealed some interesting reaction dynamics, with more than one pathway leading to the charge transfer products. The competition between short-range and long-range forces was identified as giving rise to the different charge-transfer mechanisms; when non-adiabatic coupling between the reactant and product surfaces was efficient, long-range interactions dominated and capture theory was found to describe the process well. In cases where non-adiabatic coupling was less efficient, the locations of curve crossings and subtle features on the underlying potential surfaces were found to be important—with short-range effects dominating the reaction kinetics. Perhaps most importantly, the authors noted that it was not possible to anticipate which behaviour might dominate in the absence of in-depth theoretical calculations (50).

Processes Involving Two Molecular Reactants

In addition to facilitating studies of ion-molecule reactions where one reactant is an atom, Coulomb crystals have increasingly been used to study bi-molecular reactions. Extending the advantages of sympathetic cooling to molecular ions has opened up the possibility of studying a much wider array of reactions in Coulomb crystals. There have been far fewer molecular ion-molecular neutral reaction studies so far as compared to reactions with one atomic reactant. One of the reasons for this is the added complexity of detecting multiple ionic products, as there are often several energetically accessible reaction pathways present when there are more atoms participating. There are two main detection methods that have been used to measure bi-molecular reactions in Coulomb crystals. The first involves imaging the fluorescence from the Coulomb crystal and inferring the decrease of reactant ions and increase of product ions from the shape of the crystal, aided by molecular dynamics simulations. The second uses ToF-MS to more directly measure the number of reactant and product ions as a function of reaction time. Below, we present some example reactions using both of these methods.

Indirect Reaction Product Determination

Many of the early studies of reactions between neutral molecules and molecular ions in Coulomb crystals used indirect detection methods. These methods include imaging the fluorescing laser-

cooled ions, exciting motional resonances in the crystal that depend on the mass of the trapped ions and observing the change in fluorescence, as well as more exotic methods.

The first of these methods, crystal imaging, takes advantage of the fact that the trapping potential depends inversely on the mass of the trapped ion. Thus, ions heavier than the laser-cooled species will reside farther from the center of the trap than the laser-cooled atoms; ions lighter than the laser-cooled species will reside near the trap center, displacing the laser-cooled species. This all leads to a deformation of the fluorescing laser-cooled ions within the crystal, which can be imaged and recorded with a camera. The relative numbers of the different ionic species in the trap can be inferred from these images. There are, however, limitations to this method. Primarily, it only distinguishes between ions that have either a larger or smaller mass than the laser-cooled species, but does not distinguish between two species of ions that are both lighter or heavier. Additionally, although the number of lighter ions present in a dark core can be determined quite accurately, heavier ions that sit outside the fluorescing laser-cooled ions have a much smaller impact on the shape of the crystal—making it much more challenging to determine the number of heavier ions present.

One of the first experiments to use crystal imaging to study a reaction was a multi-step “recycling reaction,” where the process started by reacting a string of Ca^+ with background O_2 to form CaO^+ (29). The presence of the molecular ions could be deduced by Ca^+ ions disappearing and dark spots appearing in the string. The next step was to introduce CO gas to the vacuum chamber. CO reacted with the CaO^+ to form trapped Ca^+ ions and CO_2 . The evidence indicating that this second reaction had taken place was seen in the reappearance of fluorescing Ca^+ ions in the string (29).

In addition to using strings of laser-cooled atoms to sympathetically cool molecular ions, full 3D crystals can be used to cool a larger number of molecular ions. An example reaction of this type started by loading OCS^+ ions into a trap that contained laser-cooled Ca^+ ions (3). As the OCS^+ ions have a higher mass than Ca^+ , they form a dark shell around the Ca^+ framework and cause a flattening of the radial edge of the crystal. Neutral, room-temperature ND_3 gas was leaked into the vacuum chamber to initiate the charge transfer reaction $\text{OCS}^+ + \text{ND}_3 \rightarrow \text{OCS} + \text{ND}_3^+$ (3). The progress of the reaction was measured by observing the appearance of a dark core in the center of the crystal, with a slight lessening of the radial distortion. These images were then compared to images created from molecular dynamics simulations to determine the number of each type of ionic species present in the trap as a function of time. This allowed for the determination of a room temperature rate coefficient (3). The experiment was repeated using a velocity-selected molecular beam of ND_3 , which enabled a rate coefficient to be determined at a translational temperature of approximately 5 K.

The control afforded by a similar Stark velocity filter was used to study reactions of sympathetically cooled N_2H^+ ions with a cold, guided beam of acetonitrile, CH_3CN (33). The beam of CH_3CN emanated from a nozzle that could be cooled down to 50 K by a cryocooler. The CH_3CN beam was then guided by an electrostatic quadrupole around two 90° bends. With a voltage of ± 3 kV applied to the rods of the quadrupole, the peak longitudinal speed of the guided CH_3CN was 34(1) m/s, which corresponded to an average collision energy with the trapped ions of 3 K. The CH_3CN beam impinged on an ion trap that contained both laser-cooled Ca^+ and N_2H^+ ions. The only energetically allowed reaction is a proton transfer reaction, which forms CH_3CNH^+ ionic products. A reaction rate was determined by measuring the disappearance of the dark core containing N_2 , assuming cylindrical symmetry in the crystal and a constant number density of neutral reactants (33).

Another related, but specialized, detection method uses a two-step process to monitor the progress of a particular class of reaction, where the only difference between the reactant and product ion is the internal rotational state. This detection method has been demonstrated in an experiment involving quantum-state selected N_2^+ ions, which were trapped along with laser-cooled Ca^+ ions (51–53). The charge transfer reaction $\text{N}_2^+ + \text{N}_2 \rightarrow \text{N}_2 + \text{N}_2^+$ was initiated by directing a molecular beam of N_2 at the trapped ions (53). The reactant and product ions were chemically identical, but the product ions were rotationally excited. To measure the number of product N_2^+ ions formed as a function of time, the product ions were optically pumped to excited vibrational states where they could react with Ar atoms also present in the vacuum chamber (53). Excited N_2^+ ions that reacted were no longer trapped in the dark core of the crystal, and so images of the crystal showed a decrease in the volume of the dark core as the reactions progressed.

Besides imaging the spatial structure of the laser-cooled species to measure ion-molecule reactions, one can use the magnitude of the fluorescence signal to gain information about the non-fluorescing ions. This method relies on the fact that the secular motional frequencies in the trap are impacted by the mass-to-charge ratios of all ions present in the crystal. To detect a change in the mass of the ions, which happens when a reaction takes place, the fluorescence from the laser-cooled ions is recorded while the trap is “shaken” at different frequencies. When this modulation approaches a motional resonance, the translational temperature of the ions increases and the magnitude of the fluorescence changes. This method has been used to measure several molecular reactions including $\text{H}_3^+ + \text{O}_2 \rightarrow \text{HO}_2^+ + \text{H}_2$ (20) and $\text{H}_3\text{O}^+ + \text{NH}_3 \rightarrow \text{NH}_4^+ + \text{H}_2$ (54).

Direct Reaction Product Determination

The previous sub-section described reaction detection methods based on imaging the fluorescence of the laser-cooled ions, with the progress of reactions monitored by measuring changes in the fluorescence pattern as a function of time. The other main class of detection methods used to monitor reactions involves ToF-MS measurements—to directly detect the products of a reaction. This is done by rapidly turning off the quadrupole trap and ejecting all the trapped ions into a ToF-MS to be able to determine the number of ions at each mass-to-charge ratio, m/z (18, 55–58). This technique allows one to track the depletion of the reactants, as well as the appearance of the charged products, over the course of the reaction. And because the m/z ratio is often a unique value for the possible reaction products (ignoring isomers, which will be discussed below), one can use the spectra to determine branching ratios and thus possible reaction pathways. This was first demonstrated for reactions involving molecular ions in a Coulomb crystal with the recording of a charge transfer and proton addition reaction (56). ToF-MS had also been used previously for atomic ion experiments (57), and has now been used to study a variety of molecular ion reaction systems.

One such set of molecular ion experiments explored the reactions of acetylene cations with two isomers of C_3H_4 , propyne and allene, to understand the impact of the isomer structure on the reaction pathways and products (59, 60). The experiments began by ionizing a neutral beam of acetylene (C_2H_2) in the center of a linear quadrupole trap before using secular excitation to eject all ions except C_2H_2^+ from the crystal. Next, an effusive beam of Ca was ionized and co-trapped with the C_2H_2^+ ions. Laser cooling reduced the temperature of the ensemble to < 1 K, where a Coulomb crystal was formed. At this point, neutral C_3H_4 was introduced into the chamber via a pulsed leak

valve to react with the trapped $C_2H_2^+$ ions. The trap was deep enough to capture all product ions, which were then sympathetically cooled via interactions with the laser-cooled Ca^+ . By varying the time between when the C_3H_4 was introduced and when the ions were ejected into the ToF-MS for detection, the progress of the reaction was able to be mapped out. Because the reaction proceeded slower than the time resolution of the measurements, the primary products were distinguished from ions formed following subsequent reactions of product ions with the excess neutral C_3H_4 present in the chamber, as can be seen in Figure 3.

For reactions with propyne, three primary ion products were formed including $C_3H_3^+$, $C_3H_4^+$, $C_5H_5^+$. However, for allene, only $C_3H_3^+$ was observed. Using the experimental identification of these product channels, along with a computed potential energy surface relevant to these reactions, it was determined that the two isomers proceeded along fundamentally different reaction pathways. For both reactions, charge exchange initiated the interaction, but this happened at different relative distances. For propyne, charge exchange happened at a short enough distance that the two reactants would form a complex that would eventually lead to the $C_5H_5^+$ product. However, for allene, charge exchange occurred at long range, which led to no complex formation. The allene cation then underwent unimolecular rearrangement to produce exclusively $C_3H_3^+$ product ions (59). These proposed mechanisms were validated by using all available hydrogen/deuterium isotopologues to see the mass shift that occurred upon deuteration (60).

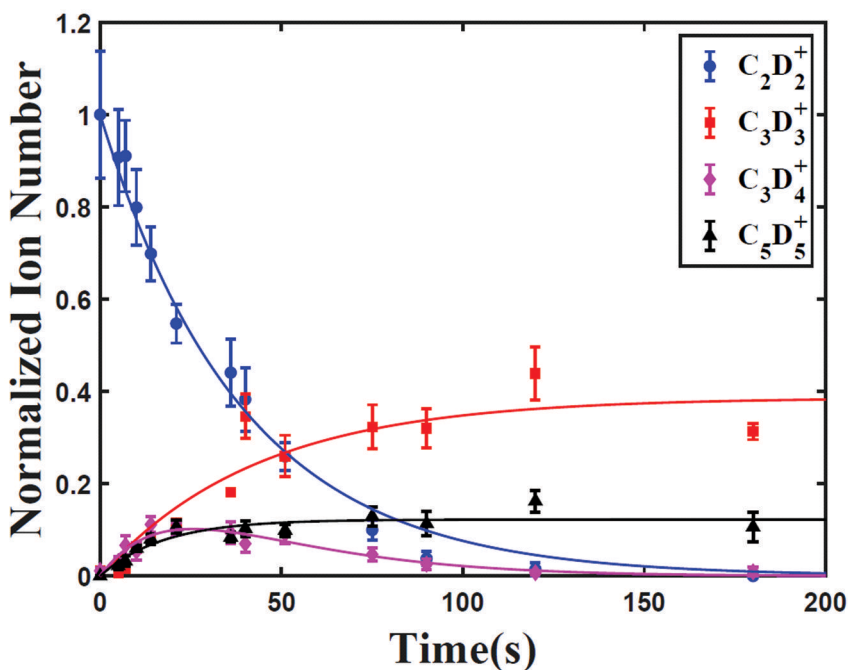


Figure 3. Primary products measured from the reaction of $C_2D_2^+ + DC_3D_3$ as a function of time. Ion numbers are normalized to the initial number of $C_2D_2^+$ in the trap. The reaction time corresponds to the amount of time propyne is in the chamber. See reference (59) for more details. Reproduced with permission from reference (59). Copyright 2020 PCCP Owner Societies.

A similar set of experiments studied the reactions of CCl^+ with neutral C_2H_2 (61) and CH_3CN (62). These experiments were facilitated by the secular excitation-induced “cleaning” of the trapped ions, as the creation of CCl^+ is accompanied by a significant number of contaminant ions. For both of these reactions, reaction pathways were proposed and branching ratios were measured. While rate coefficients were also reported, there is some uncertainty associated with the rate coefficient measurements, as the concentration of the neutral gas was measured with an ion gauge, which has well-known calibration issues at the pressures used ($\sim 10^{-9}$ torr). This calibration challenge limits the accuracy of the determination of rate coefficients for many of these types of trapped ion reaction measurements.

Finally, another experiment that took advantage of direct detection of product ions explored how different nuclear-spin isomers of H_2O reacted with sympathetically cooled N_2H^+ ions (63). A beam of H_2O seeded in argon was created via pulsed supersonic expansion, with population concentrated in the lowest two rotational states of the vibrational ground state. The ground and first excited rotational states have different nuclear spin; the absolute ground state is para-water and the first rotationally excited state is ortho-water. The beam was then sent through an electrostatic deflector that deflected the two states by different amounts, due to their different Stark shifts. The deflected beam was directed towards a ion trap containing laser-cooled Ca^+ ions and sympathetically cooled N_2H^+ ions, which was coupled to a ToF-MS. By adjusting the angle of the molecular beam apparatus with respect to the ion trap, the relative fraction of ortho-water to para-water could be changed. Therefore, by measuring both the depletion of N_2H^+ reactants and the appearance of H_3O^+ product ions as the ratio of the two isomers changed in the beam, reaction rate coefficients were determined for both states. Through careful measurements and modeling of the molecular beam parameters, it was determined that the para-isomer reacted 23(9)% faster than the ortho-isomer. This was the first demonstration of reactions with rotationally state-selected polyatomic molecules and trapped ions conducted in a Coulomb crystal.

Spectroscopic Studies

Traditionally, laser-based spectroscopic methods have involved the recording of absorption or fluorescence spectra. These sorts of measurements are not practical for precise studies of trapped molecular ions in Coulomb crystals, as there are too few molecular ions present. Detecting absorption or fluorescence from a sample of only a few hundred ions (where the population may be spread over tens of different quantum states) is beyond the sensitivity limit of most detectors. While performing direct absorption or fluorescence spectroscopic measurements is not feasible, action spectroscopy allows infrequent events (or low signal levels) to be detected with high efficiency. In the most general terms, an action spectrum measures the likelihood of a certain outcome—induced by a photon-driven process—as a function of photon wavelength. For the applications described in this chapter, action spectroscopy generally involves monitoring product formation (where the product is chemically distinct from the parent species that absorbs the photon). Action spectra are frequently recorded using complementary detection methods, such as ToF-MS or crystal imaging, and can provide a highly sensitive means of probing the trapped ions of interest.

Although the number of ions is limited in Coulomb crystals, the high degree of localisation of ions, the long trapping lifetimes, and the largely inert environment are ideal for sensitive spectroscopic measurements. The potential applications of spectroscopic measurements in this setting are wide-ranging—spanning the fundamental understanding of molecular properties, to

identifying spectroscopic transitions in astrochemically relevant species, to quantum logic spectroscopy. In this section, we provide an overview of the key spectroscopic techniques employed to probe ions in Coulomb crystals. The discussion builds upon the groundwork laid by earlier reviews (9, 10), with a focus on some recent results and exciting new developments.

Identifying Molecular Properties

Laser-Induced Reactions

Lasers can be employed to initiate chemical reactions in Coulomb crystals, and in doing so can facilitate spectroscopic measurements. For example, an endothermic ion-molecule reaction (i.e., a process that is energetically forbidden for ground-state ions) can become energetically allowed if the reactant ions are promoted to an excited state. As molecular ions will be excited only when the laser frequency is resonant with the frequency of a transition, laser-induced reactions can (indirectly) establish the frequencies of spectroscopic transitions in trapped molecular ions. While this approach has been utilised for a range of molecular ions in multipole traps, it has only been applied to species such as N_2^+ in Coulomb crystals. The primary reason for the limited use of laser-induced reaction spectroscopic measurements is because it is very difficult to control the internal quantum-state distribution of most molecular ions in Coulomb crystals.

A central requirement of any laser-induced reaction spectroscopy implementation is that the molecular ions must initially be in a low-energy state (typically in the ground vibrational level of the ground electronic state)—else the reaction could proceed without laser excitation. This is easily achieved for homonuclear diatomic ions that can be formed in a state-selective manner, such as H_2^+ and N_2^+ , but is challenging to implement for most other molecular ions in Coulomb crystals. As highlighted in the introduction to this chapter, sympathetic cooling of co-trapped ions occurs due to elastic collisions with laser-cooled atomic ions. This method is effective at cooling the translational degrees of freedom of molecular ions, enabling them to be spatially confined and incorporated into Coulomb crystals. However, long-range Coulomb interactions inhibit short-range encounters; no inelastic collisions (which change the internal states of the ion) occur between co-trapped ions in Coulomb crystals. Even molecular ions that are formed in a state-selective manner typically exhibit a thermal rovibrational state distribution within tens of seconds (65, 66). This is due to interactions with the ambient blackbody radiation (BBR) field. Only those molecular ions that do not interact with BBR—such as homonuclear diatomics—retain their initially prepared population distribution. With the introduction of a number of cryogenic ion trap chambers designed to operate at temperatures < 10 K (67–70), it is anticipated that maintaining state selectivity in a broad range of molecular ions will be feasible in the near future. (See (10) for a discussion on some of the other existing approaches to controlling the rotational state distribution of trapped molecular ions.)

The N_2^+ ion is one species that has been successfully probed spectroscopically using laser-induced reactions. N_2^+ ions were state-selectively formed in the rovibronic ground state following the $(2 + 1)$ REMPI of N_2 . The molecular ions were subsequently sympathetically cooled and incorporated into the center of a Ca^+ Coulomb crystal. A mid-IR quantum-cascade laser was directed into the ion trap to excite the electric-quadrupole vibrational transition in N_2^+ and Ar gas was admitted into the vacuum chamber to react with the excited N_2^+ (64). The number of N_2^+ ions excited at a selected laser frequency was identified by monitoring the loss of N_2^+ ions from

the crystal as a function of IR laser wavelength. Only vibrationally-excited N_2^+ ions could undergo charge transfer reactions with Ar, meaning that N_2^+ ions were only lost from the crystal when the IR laser was resonant with a vibrational transition. In this way, the hyperfine components of a dipole-forbidden, electric-quadrupole-allowed transition in N_2^+ were able to be precisely established for the first time (see Figure 4) (64).

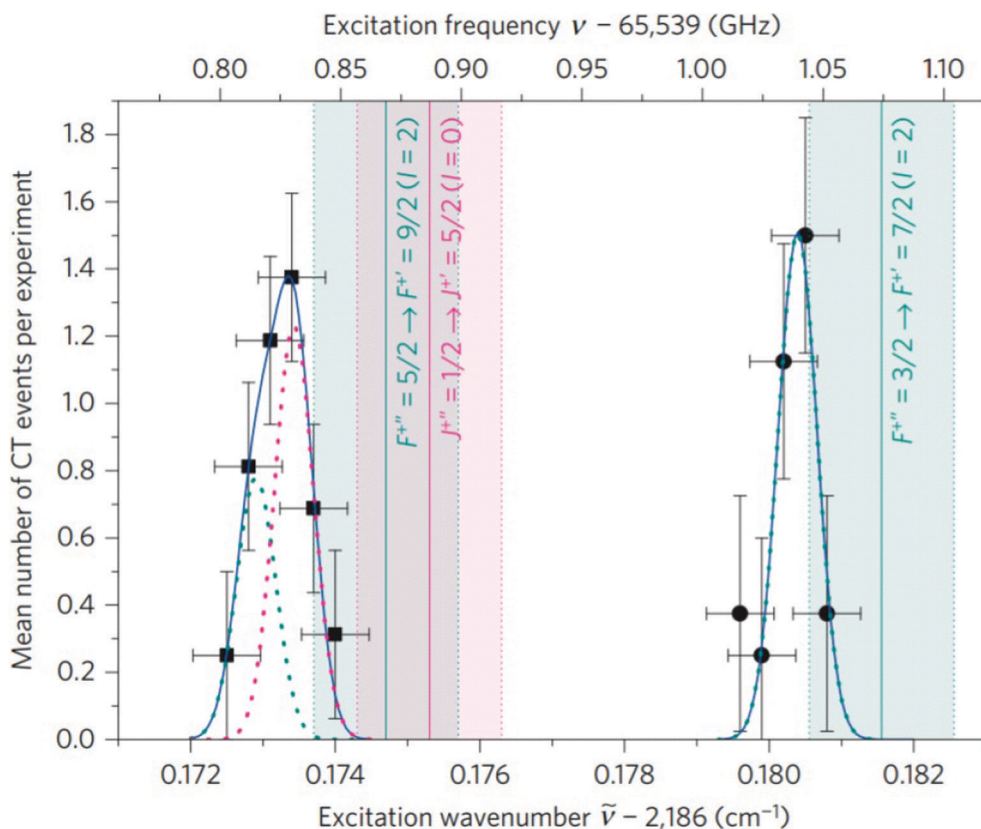


Figure 4. The locations of hyperfine components of electric-dipole-forbidden transitions in ortho- N_2^+ are shown, as established from the mean number of charge-transfer reactions that occurred as a function of excitation frequency. Experimental data points are indicated by solid squares/circles, with error bars indicating the uncertainty in the measurements. Dotted lines indicate Gaussian fits to the three transitions identified, with the sum of these Gaussians shown as a solid line. Vertical lines represent theoretical predictions of the transitions, with the shaded regions illustrating the uncertainty in these calculations. See reference (64) for more details. Reproduced with permission from reference (64). Copyright 2014 Nature Publishing Group.

Resonance-Enhanced Multiphoton Dissociation, REMPD

Resonance-enhanced multiphoton dissociation (REMPD) schemes have been employed to spectroscopically probe molecular ions in Coulomb crystals. The operating principle of REMPD is similar to that seen in REMPI schemes—with the key difference being that the species of interest is resonantly dissociated with REMPD (rather than ionised, as occurs with REMPI schemes). Spectroscopic transitions are identified by monitoring either the loss of dark ions (when the product

ion, such as H^+ , cannot be confined by the trapping fields) or the change in the mass of the trapped ions (if the product ions are subsequently trapped) as a function of the REMPD laser frequency. When the molecular ion of interest is resonantly dissociated, the loss of the parent ion can be sensitively detected through imaging methods (frequently combined with molecular dynamics simulations). REMPD spectroscopic measurements have been successfully undertaken for trapped ensembles of MgH^+ and CaH^+ ions, in Coulomb crystals containing as few as two ions and up to several thousand ions (67, 71).

REMPD measurements have enabled the rotational state distribution of an ensemble of Coulomb-crystallised MgH^+ ions held in a cryogenic trap to be established, under a range of different of experimental conditions. Inelastic collisions with helium buffer gas efficiently cooled the rotational degrees of freedom of the molecular ions, even though the helium collision rate was very low (10 s^{-1}). By adjusting the properties of the Coulomb crystals, it was demonstrated that the rotational state distribution of trapped MgH^+ ions could be tuned from 7 to 60 K (67).

A rather different approach was employed to probe single CaH^+ ions co-trapped with two laser-cooled Ca^+ ions. A two-photon photodissociation scheme first excited a vibrational overtone of CaH^+ , before the molecular ion was photodissociated into $\text{Ca}^+ + \text{H}$ fragments by the second photon. Thanks to multiple repeats and control experiments, two weak vibrational overtone transitions were able to be experimentally identified in CaH^+ for the first time. The REMPD process was monitored by considering the change in the Ca^+ fluorescence signal as the frequency of the first laser was scanned. With only three trapped ions involved, the laser-induced dissociation process could be monitored on a single-ion level: the dissociation of a single (dark) CaH^+ ion to yield a (fluorescing) Ca^+ ion was observed (71). Subsequent REMPD studies on calcium hydride molecular ions in Ca^+ Coulomb crystals have seen a number of additional rovibronic transitions identified in the past few years (9, 72, 73). Indeed, the identification of vibronic transitions in CaD^+ resulted in the re-assignment of previously observed vibronic transitions in CaH^+ . The transitions in CaH^+ were initially mis-assigned based on theoretical calculations—numbers that have subsequently been found to disagree with experimental values by some 700 cm^{-1} (72, 73). These findings highlight the importance of detailed investigations when assigning spectroscopic transitions, and the power of REMPD experimental measurements.

Finally, a related (but non-resonant) technique, termed photodissociation thermometry, was introduced in 2013 to establish the vibrational-state population distribution of Coulomb-crystallised BaCl^+ ions. The method employed broadband photodissociation of BaCl^+ to produce $\text{Ba}^+ + \text{Cl}$, as there was insufficient spectroscopic information about the molecular ion for resonance-enhanced dissociation techniques to be implemented. The photodissociation thermometry method enabled the relative populations of the vibrational levels of BaCl^+ ions to be estimated under different experimental conditions—confirming that vibrational degrees of freedom can be quenched by collisions with laser-cooled atoms in a hybrid trap (74).

Additional Laser-Based Coulomb Crystal Experiments

There have been a diverse range of other spectroscopy-related measurements performed with Coulomb crystals (9, 10). As it is not practical to discuss all of these experiments in this book chapter, several studies that are most relevant to physical chemistry and chemical physics have been highlighted in the preceding subsections. Other active areas of research include quantum logic

spectroscopy (75, 76), laser cooling of molecular (AlH^+) ions using a broadband laser source (77), laser-driven BBR-mediated population redistribution in molecular ions (78, 79), Doppler-free spectroscopy (80), and frequency-comb-driven Raman transitions in atomic ions (81).

Future Prospects

There are many advantages associated with measurements using trapped ions in Coulomb crystals. A high degree of control can be exerted over the experimental conditions and processes can be studied with exceptional sensitivity—for both reaction studies and spectroscopic measurements. The experiments discussed above highlight some of the applications that have been explored using Coulomb crystals. This body of work has improved our understanding of fundamental molecular properties and reaction processes, has facilitated critical tests of the accuracy of PESs and theories of reactivity, and has seen measurements undertaken with direct relevance to gas-phase environments such as the ISM. The field is still emerging, with new experimental methods, new combinations of techniques, and new applications likely to be introduced in the coming years. The future prospects for chemistry with Coulomb crystals are therefore both exciting and wide-reaching.

In particular, new combinations of existing experimental techniques (such as the interfacing of cold neutral molecule sources with ion traps) will expand the range of reaction systems that can be examined under cold and controlled conditions. Improvements in detection sensitivity will enable very infrequent events to be observed. The development of a number of cryogenic linear Paul traps (see, for example (67–70),) will allow for improved control over the quantum state population distribution of trapped molecular ions. Finally, sustained interest in the field of quantum computing will likely see further growth in areas such as quantum logic spectroscopy.

There are also some potential future directions that are rather less obvious (and perhaps less certain), but which still warrant mentioning here. An open question for the field is whether the methods described above—implemented for Coulomb crystals composed of cations—can be extended to anions. While laser cooling schemes have been developed for a number of neutral atoms and atomic cations, along with a handful of molecular species, laser cooling is yet to be successfully applied to an anionic species. This is primarily due to there being few (if any) bound excited electronic states in most atomic anions; as the excess electron is only weakly bound, the threshold energy for photodetachment of the electron is often very low. Three atomic anions identified as possible candidates for laser cooling include Os^- , La^- and Ce^- (82–85). Potential laser cooling schemes have also been proposed for the diatomic carbon anion, C_2^- , as a number of bound electronic states are known to lie below the energetic threshold for photodetachment (86, 87). If laser cooling can be achieved for one or more of these anions, this could enable Coulomb crystals to be formed—and could see the methods outlined above applied to anionic species for the first time.

References

1. Bruzewicz, C. D.; Chiaverini, J.; McConnell, R.; Sage, J. M. Trapped-ion quantum computing: Progress and challenges. *Applied Physics Reviews* **2019**, *6*, 021314.
2. Willitsch, S.; Bell, M. T.; Gingell, A. D.; Softley, T. P. Chemical applications of laser-and sympathetically-cooled ions in ion traps. *Physical Chemistry Chemical Physics* **2008**, *10*, 7200–7210.

3. Bell, M. T.; Gingell, A. D.; Oldham, J. M.; Softley, T. P.; Willitsch, S. Ion-molecule chemistry at very low temperatures: cold chemical reactions between Coulomb-crystallized ions and velocity-selected neutral molecules. *Faraday Discussions* **2009**, *142*, 73–91.
4. Willitsch, S. Coulomb-crystallised molecular ions in traps: methods, applications, prospects. *International Reviews in Physical Chemistry* **2012**, *31*, 175–199.
5. Thompson, R. C. Ion Coulomb crystals. *Contemporary Physics* **2015**, *56*, 63–79.
6. Heazlewood, B. R.; Softley, T. P. Low-temperature kinetics and dynamics with Coulomb crystals. *Annual Review of Physical Chemistry* **2015**, *66*, 475–495.
7. Drewsen, M. Ion Coulomb crystals. *Physica B: Condensed Matter* **2015**, *460*, 105–113.
8. Willitsch, S. Chemistry with controlled ions. *Adv. Chem. Phys* **2017**, *162*, 307–340.
9. Calvin, A. T.; Brown, K. R. Spectroscopy of molecular ions in Coulomb crystals. *The Journal of Physical Chemistry Letters* **2018**, *9*, 5797–5804.
10. Heazlewood, B. R. Cold ion chemistry within Coulomb crystals. *Molecular Physics* **2019**, *117*, 1934–1941.
11. Toscano, J.; Lewandowski, H. J.; Heazlewood, B. R. Cold and controlled chemical reaction dynamics. *Physical Chemistry Chemical Physics* **2020**, *22*, 9180–9194.
12. Heazlewood, B. R.; Softley, T. P. Towards chemistry at absolute zero. *Nature Reviews Chemistry* **2021**, *5*, 125–140.
13. Pollock, E. L.; Hansen, J.-P. Statistical mechanics of dense ionized matter. II. Equilibrium properties and melting transition of the crystallized one-component plasma. *Physical Review A* **1973**, *8*, 3110.
14. Slattery, W. L.; Doolen, G. D.; DeWitt, H. E. Improved equation of state for the classical one-component plasma. *Physical Review A* **1980**, *21*, 2087.
15. Neuhauser, W.; Hohenstatt, M.; Toschek, P.; Dehmelt, H. Optical-sideband cooling of visible atom cloud confined in parabolic well. *Physical Review Letters* **1978**, *41*, 233.
16. Wineland, D. J.; Drullinger, R. E.; Walls, F. L. Radiation-pressure cooling of bound resonant absorbers. *Physical Review Letters* **1978**, *40*, 1639.
17. Eschner, J.; Morigi, G.; Schmidt-Kaler, F.; Blatt, R. Laser cooling of trapped ions. *JOSA B* **2003**, *20*, 1003–1015.
18. Meyer, K. A. E.; Pollum, L. L.; Petralia, L. S.; Tauschinsky, A.; Rennick, C. J.; Softley, T. P.; Heazlewood, B. R. Ejection of Coulomb Crystals from a Linear Paul Ion Trap for Ion–Molecule Reaction Studies. *The Journal of Physical Chemistry A* **2015**, *119*, 12449–12456.
19. Mølhave, K.; Drewsen, M. Formation of translationally cold MgH⁺ and MgD⁺ molecules in an ion trap. *Physical Review A* **2000**, *62*, 011401.
20. Roth, B.; Blythe, P.; Wenz, H.; Daerr, H.; Schiller, S. Ion-neutral chemical reactions between ultracold localized ions and neutral molecules with single-particle resolution. *Physical Review A* **2006**, *73*, 042712.
21. Gingell, A. D.; Bell, M. T.; Oldham, J. M.; Softley, T. P.; Harvey, J. N. Cold chemistry with electronically excited Ca⁺ Coulomb crystals. *The Journal of Chemical Physics* **2010**, *133*, 194302.
22. Yang, T.; Li, A.; Chen, G. K.; Xie, C.; Suits, A. G.; Campbell, W. C.; Guo, H.; Hudson, E. R. Optical control of reactions between water and laser-cooled Be⁺ ions. *The Journal of Physical Chemistry Letters* **2018**, *9*, 3555–3560.

23. Greenberg, J.; Schmid, P. C.; Miller, M.; Stanton, J. F.; Lewandowski, H. J. Quantumstate-controlled reactions between molecular radicals and ions. *Physical Review A* **2018**, *98*, 032702.
24. Schmid, P. C.; Miller, M. I.; Greenberg, J.; Nguyen, T. L.; Stanton, J. F.; Lewandowski, H. J. Quantum-state-specific reaction rate measurements for the photo-induced reaction $\text{Ca}^+ + \text{O}_2 \rightarrow \text{CaO}^+ + \text{O}$. *Molecular Physics* **2019**, *117*, 3036–3042.
25. Saito, R.; Haze, S.; Sasakawa, M.; Nakai, R.; Raoult, M.; Da Silva, H., Jr; Dulieu, O.; Mukaiyama, T. Characterization of charge-exchange collisions between ultracold ^6Li atoms and $^4\text{Ca}^+$ ions. *Physical Review A* **2017**, *95*, 032709.
26. Li, H.; Jyothi, S.; Li, M.; Kłos, J.; Petrov, A.; Brown, K. R.; Kotochigova, S. Photonmediated charge exchange reactions between ^{39}K atoms and $^{40}\text{Ca}^+$ ions in a hybrid trap. *Physical Chemistry Chemical Physics* **2020**, *22*, 10870–10881.
27. Hall, F. H. J.; Aymar, M.; Bouloufa-Maafa, N.; Dulieu, O.; Willitsch, S. Light-assisted ion-neutral reactive processes in the cold regime: Radiative molecule formation versus charge exchange. *Physical Review Letters* **2011**, *107*, 243202.
28. Kimura, N.; Okada, K.; Takayanagi, T.; Wada, M.; Ohtani, S.; Schuessler, H. A. Sympathetic crystallization of CaH^+ produced by a laser-induced reaction. *Physical Review A* **2011**, *83*, 033422.
29. Drewsen, M.; Hornekær, L.; Kjærgaard, N.; Mølhave, K.; Thommesen, A.-M.; Videsen, Z.; Mortensen, A.; Jensen, F. Ion Coulomb crystals and some applications. *AIP Conference Proceedings* **2002**, *606*, 135–144.
30. Okada, K.; Wada, M.; Boesten, L.; Nakamura, T.; Katayama, I.; Ohtani, S. Acceleration of the chemical reaction of trapped Ca^+ ions with H_2O molecules by laser excitation. *Journal of Physics B: Atomic, Molecular and Optical Physics* **2002**, *36*, 33.
31. Chen, G. K.; Xie, C.; Yang, T.; Li, A.; Suits, A. G.; Hudson, E. R.; Campbell, W. C.; Guo, H. Isotope-selective chemistry in the $\text{Be}^+(^2\text{S}_{1/2}) + \text{HOD} \rightarrow \text{BeOD}^+/\text{BeOH}^+ + \text{H/D}$ reaction. *Physical Chemistry Chemical Physics* **2019**, *21*, 14005–14011.
32. Rösch, D.; Gao, H.; Kilaj, A.; Willitsch, S. Design and characterization of a linear quadrupole ion trap for high-resolution Coulomb-crystal time-of-flight mass spectrometry. *EPJ Techniques and Instrumentation* **2016**, *3*, 1–14.
33. Okada, K.; Suganuma, T.; Furukawa, T.; Takayanagi, T.; Wada, M.; Schuessler, H. A. Cold ion–polar-molecule reactions studied with a combined Stark-velocity-lter-ion-trap apparatus. *Physical Review A* **2013**, *87*, 043427.
34. Chang, Y.-P.; Długołęcki, K.; Küpper, J.; Rösch, D.; Wild, D.; Willitsch, S. Specific chemical reactivities of spatially separated 3-aminophenol conformers with cold Ca^+ ions. *Science* **2013**, *342*, 98–101.
35. Roth, B.; Offenberg, D.; Zhang, C. B.; Schiller, S. Chemical reactions between cold trapped Ba^+ ions and neutral molecules in the gas phase. *Physical Review A* **2008**, *78*, 042709.
36. DePalatis, M. V.; Chapman, M. S. Production of translationally cold barium monohalide ions. *Physical Review A* **2013**, *88*, 023403.
37. Puri, P.; Mills, M.; Schneider, C.; Simbotin, I.; Montgomery, J. A.; Côté, R.; Suits, A. G.; Hudson, E. R. Synthesis of mixed hypermetallic oxide BaOCa^+ from lasercooled reagents in an atom-ion hybrid trap. *Science* **2017**, *357*, 1370–1375.

38. Joger, J.; Fürst, H.; Ewald, N.; Feldker, T.; Tomza, M.; Gerritsma, R. Observation of collisions between cold Li atoms and Yb⁺ ions. *Physical Review A* **2017**, *96*, 030703.
39. Rellergert, W. G.; Sullivan, S. T.; Kotochigova, S.; Petrov, A.; Chen, K.; Schowalter, S. J.; Hudson, E. R. Measurement of a Large Chemical Reaction Rate between Ultracold Closed-Shell ⁴⁰Ca Atoms and Open-Shell ¹⁷⁴Yb⁺ Ions Held in a Hybrid Atom-Ion Trap. *Physical Review Letters* **2011**, *107*, 243201.
40. Ratschbacher, L.; Zipkes, C.; Sias, C.; Köhl, M. Controlling chemical reactions of a single particle. *Nature Physics* **2012**, *8*, 649–652.
41. Fan, M.; Holliman, C. A.; Shi, X.; Zhang, H.; Straus, M. W.; Li, X.; Buechele, S. W.; Jayich, A. M. Optical mass spectrometry of cold RaOH⁺ and RaOCH₃⁺. *Physical Review Letters* **2021**, *126*, 023002.
42. Drewsen, M.; Jensen, I.; Lindballe, J.; Nissen, N.; Martinussen, R.; Mortensen, A.; Staunum, P.; Voigt, D. Ion Coulomb crystals: a tool for studying ion processes. *International Journal of Mass Spectrometry* **2003**, *229*, 83–91.
43. Okada, K.; Sakimoto, K.; Takada, Y.; Schuessler, H. A. A study of the translational temperature dependence of the reaction rate constant between CH₃CN and Ne⁺ at low temperatures. *The Journal of Chemical Physics* **2020**, *153*, 124305.
44. Petralia, L. S.; Tsikritea, A.; Loreau, J.; Softley, T. P.; Heazlewood, B. R. Strong inverse kinetic isotope effect observed in ammonia charge exchange reactions. *Nature Communications* **2020**, *11*, 173.
45. Tsikritea, A.; Park, K.; Bertier, P.; Loreau, J.; Softley, T. P.; Heazlewood, B. R. Inverse kinetic isotope effects in the charge transfer reactions of ammonia with rare gas ions. *Chemical Science* **2021**, *12*, 10005–10013.
46. Yang, T.; Li, A.; Chen, G. K.; Yao, Q.; Suits, A. G.; Guo, H.; Hudson, E. R.; Campbell, W. C. Isomer-specific kinetics of the C⁺+ H₂O reaction at the temperature of interstellar clouds. *Science Advances* **2021**, *7*, eabe4080.
47. Tomza, M.; Jachymski, K.; Gerritsma, R.; Negretti, A.; Calarco, T.; Idziaszek, Z.; Julienne, P. S. Cold hybrid ion-atom systems. *Reviews of Modern Physics* **2019**, *91*, 035001.
48. Oates, C. W.; Bondu, F.; Fox, R. W.; Hollberg, L. A diode-laser optical frequency standard based on laser-cooled Ca atoms: Sub-kilohertz spectroscopy by optical shelving detection. *The European Physical Journal D-Atomic, Molecular, Optical and Plasma Physics* **1999**, *7*, 449–460.
49. Puri, P.; Mills, M.; Simbotin, I.; Montgomery, J. A.; Côté, R.; Schneider, C.; Suits, A. G.; Hudson, E. R. Reaction blockading in a reaction between an excited atom and a charged molecule at low collision energy. *Nature Chemistry* **2019**, *11*, 615–621.
50. Dörfler, A. D.; Eberle, P.; Koner, D.; Tomza, M.; Meuwly, M.; Willitsch, S. Long-range versus short-range effects in cold molecular ion-neutral collisions. *Nature Communications* **2019**, *10*, 5429.
51. Tong, X.; Winney, A. H.; Willitsch, S. Sympathetic Cooling of Molecular Ions in Selected Rotational and Vibrational States Produced by Threshold Photoionization. *Physical Review Letters* **2010**, *105*, 143001.

52. Tong, X.; Wild, D.; Willitsch, S. Collisional and radiative effects in the state-selective preparation of translationally cold molecular ions in ion traps. *Physical Review A* **2011**, *83*, 023415.
53. Tong, X.; Nagy, T.; Reyes, J. Y.; Germann, M.; Meuwly, M.; Willitsch, S. State-selected ion–molecule reactions with Coulomb-crystallized molecular ions in traps. *Chemical Physics Letters* **2012**, *547*, 1–8.
54. Baba, T.; Waki, I. Chemical reaction of sympathetically laser-cooled molecular ions. *The Journal of Chemical Physics* **2002**, *116*, 1858–1861.
55. Schmid, P. C.; Greenberg, J.; Miller, M. I.; Loeffler, K.; Lewandowski, H. J. An ion trap time-of-flight mass spectrometer with high mass resolution for cold trapped ion experiments. *Review of Scientific Instruments* **2017**, *88*, 123107.
56. Deb, N.; Pollum, L. L.; Smith, A. D.; Keller, M.; Rennick, C. J.; Heazlewood, B. R.; Softley, T. P. Coulomb crystal mass spectrometry in a digital ion trap. *Physical Review A* **2015**, *91*, 033408.
57. Schowalter, S. J.; Chen, K.; Rellergert, W. G.; Sullivan, S. T.; Hudson, E. R. An integrated ion trap and time-of-flight mass spectrometer for chemical and photo-reaction dynamics studies. *Review of Scientific Instruments* **2012**, *83*, 043103.
58. Rösch, D.; Gao, H.; Kilaj, A.; Willitsch, S. Design and characterization of a linear quadrupole ion trap for high-resolution Coulomb-crystal time-of-flight mass spectrometry. *EPJ Techniques and Instrumentation* **2016**, *3*, 5.
59. Schmid, P. C.; Greenberg, J.; Nguyen, T. L.; Thorpe, J. H.; Catani, K. J.; Krohn, O. A.; Miller, M. I.; Stanton, J. F.; Lewandowski, H. J. Isomer-selected ion–molecule reactions of acetylene cations with propyne and allene. *Physical Chemistry Chemical Physics* **2020**, *22*, 20303–20310.
60. Greenberg, J.; Schmid, P. C.; Thorpe, J. H.; Nguyen, T. L.; Catani, K. J.; Krohn, O. A.; Miller, M. I.; Stanton, J. F.; Lewandowski, H. J. Using isotopologues to probe the potential energy surface of reactions of $C_2H_2^+ + C_3H_4$. *The Journal of Chemical Physics* **2021**, *154*, 124310.
61. Catani, K. J.; Greenberg, J.; Saarel, B. V.; Lewandowski, H. J. Reactions of translationally cold trapped CCl^+ with acetylene (C_2H_2). *The Journal of Chemical Physics* **2020**, *152*, 234310.
62. Krohn, O. A.; Catani, K. J.; Greenberg, J.; Sundar, S. P.; da Silva, G.; Lewandowski, H. J. Isotope-specific reactions of acetonitrile (CH_3CN) with trapped, translationally cold CCl^+ . *The Journal of Chemical Physics* **2021**, *154*, 074305.
63. Kilaj, A.; Gao, H.; Rösch, D.; Rivero, U.; Küpper, J.; Willitsch, S. Observation of different reactivities of para and ortho-water towards trapped diazenylium ions. *Nature Communications* **2018**, *9*, 1–7.
64. Germann, M.; Tong, X.; Willitsch, S. Observation of electric-dipole-forbidden infrared transitions in cold molecular ions. *Nature Physics* **2014**, *10*, 820–824.
65. Deb, N.; Heazlewood, B. R.; Bell, M. T.; Softley, T. P. Blackbody-mediated rotational laser cooling schemes in MgH^+ , DCl^+ , HCl^+ , LiH and CsH . *Physical Chemistry Chemical Physics* **2013**, *15*, 14270–14281.
66. Deb, N.; Heazlewood, B. R.; Rennick, C. J.; Softley, T. P. Laser induced rovibrational cooling of the linear polyatomic ion $C_2H_2^+$. *The Journal of Chemical Physics* **2014**, *140*, 164314.

67. Hansen, A. K.; Versolato, O. O.; Kłosowski, L.; Kristensen, S. B.; Gingell, A.; Schwarz, M.; Windberger, A.; Ullrich, J.; López-Urrutia, J. R. C.; Drewsen, M. Efficient rotational cooling of Coulomb-crystallized molecular ions by a helium buffer gas. *Nature* **2014**, *508*, 76–79.
68. Schwarz, M.; Versolato, O. O.; Windberger, A.; Brunner, F. R.; Ballance, T.; Eberle, S. N.; Ullrich, J.; Schmidt, P. O.; Hansen, A. K.; Gingell, A. D.; Drewsen, M.; Crespo López-Urrutia, J. R. Cryogenic linear Paul trap for cold highly charged ion experiments. *Review of Scientific Instruments* **2012**, *83*, 083115.
69. Leopold, T.; King, S. A.; Micke, P.; Bautista-Salvador, A.; Heip, J. C.; Ospelkaus, C.; Crespo López-Urrutia, J. R.; Schmidt, P. O. A cryogenic radio-frequency ion trap for quantum logic spectroscopy of highly charged ions. *Review of Scientific Instruments* **2019**, *90*, 073201.
70. Hejduk, M.; Heazlewood, B. R. Off-axis parabolic mirror relay microscope for experiments with ultra-cold matter. *Review of Scientific Instruments* **2019**, *90*, 123701.
71. Khanyile, N. B.; Shu, G.; Brown, K. R. Observation of vibrational overtones by single-molecule resonant photodissociation. *Nature Communications* **2015**, *6*, 7825.
72. Rugango, R.; Calvin, A. T.; Janardan, S.; Shu, G.; Brown, K. R. Vibronic Spectroscopy of Sympathetically Cooled CaH⁺. *ChemPhysChem* **2016**, *17*, 3764–3768.
73. Condoluci, J.; Janardan, S.; Calvin, A.; Rugango, R.; Shu, G.; Sherrill, C.; Brown, K. Reassigning the CaH⁺ $1^1\Sigma \rightarrow 2^1\Sigma$ vibronic transition with CaD⁺. *The Journal of Chemical Physics* **2017**, *147*, 214309.
74. Rellergert, W. G.; Sullivan, S. T.; Schowalter, S. J.; Kotochigova, S.; Chen, K.; Hudson, E. R. Evidence for sympathetic vibrational cooling of translationally cold molecules. *Nature* **2013**, *495*, 490–494.
75. Chou, C.-w.; Kurz, C.; Hume, D. B.; Plessow, P. N.; Leibbrandt, D. R.; Leibfried, D. Preparation and coherent manipulation of pure quantum states of a single molecular ion. *Nature* **2017**, *545*, 203.
76. Wolf, F.; Wan, Y.; Heip, J. C.; Gebert, F.; Shi, C.; Schmidt, P. O. Non-destructive state detection for quantum logic spectroscopy of molecular ions. *Nature* **2016**, *530*, 457–460.
77. Lien, C.-Y.; Seck, C. M.; Yen-Wei Lin, J. H. N.; Tabor, D. A.; Odom, B. C. Broadband optical cooling of molecular rotors from room temperature to the ground state. *Nature Communications* **2014**, *5*, 4783.
78. Sta anum, P. F.; Højbjerg, K.; Skyt, P. S.; Hansen, A. K.; Drewsen, M. Rotational laser cooling of vibrationally and translationally cold molecular ions. *Nature Physics* **2010**, *6*, 271–274.
79. Schneider, T.; Roth, B.; Duncker, H.; Ernsting, I.; Schiller, S. All-optical preparation of molecular ions in the rovibrational ground state. *Nature Physics* **2010**, *6*, 275–278.
80. Alighanbari, S.; Hansen, M. G.; Korobov, V.; Schiller, S. Rotational spectroscopy of cold and trapped molecular ions in the Lamb–Dicke regime. *Nature Physics* **2018**, *14*, 555–559.
81. Solaro, C.; Meyer, S.; Fisher, K.; DePalatis, M. V.; Drewsen, M. Direct Frequency-Comb-Driven Raman Transitions in the Terahertz Range. *Physical Review Letters* **2018**, *120*, 253601.
82. Kellerbauer, A.; Fischer, A.; Warring, U. Measurement of the Zeeman effect in an atomic anion: Prospects for laser cooling of Os⁻. *Physical Review A* **2014**, *89*, 043430.
83. Pan, L.; Beck, D. R. Candidates for laser cooling of atomic anions: La⁻ versus Os⁻. *Physical Review A* **2010**, *82*, 014501.

84. Walter, C.; Gibson, N.; Li, Y.-G.; Matyas, D.; Alton, R.; Lou, S.; Field III, R.; Hanstorp, D.; Pan, L.; Beck, D. R. Experimental and theoretical study of bound and quasibound states of Ce^- . *Physical Review A* **2011**, *84*, 032514.
85. Walter, C.; Gibson, N.; Matyas, D.; Crocker, C.; Dungan, K.; Matola, B.; Rohlén, J. Candidate for laser cooling of a negative ion: observations of bound-bound transitions in La^- . *Physical Review Letters* **2014**, *113*, 063001.
86. Yzombard, P.; Hamamda, M.; Gerber, S.; Doser, M.; Comparat, D. Laser cooling of molecular anions. *Physical Review Letters* **2015**, *114*, 213001.
87. Mant, B. P.; Gianturco, F. A.; Wester, R.; Yurtsever, E.; González-Sánchez, L. Rovibrational quenching of C_2^- anions in collisions with He, Ne, and Ar atoms. *Physical Review A* **2020**, *102*, 062810.